

## Growth kinetics of $\text{CaF}_2/\text{Si}(111)$ for a two-step deposition

Andreas Klust,<sup>\*</sup> Robert Kayser, and Joachim Wollschläger

*Institut für Festkörperphysik, Universität Hannover Appelstraße 2, D-30167 Hannover, Germany*

(Received 14 December 1999)

The growth of  $\text{CaF}_2$  on vicinal  $\text{Si}(111)$  substrates precovered by an interfacial  $\text{CaF}$  layer was investigated using atomic force microscopy (AFM). The interfacial  $\text{CaF}$  layer is grown in a first deposition step at  $750^\circ\text{C}$ , depositing 1.3 triple layers (TL's)  $\text{CaF}_2$ . This is partially covered by  $\text{CaF}_2$  due to the deposition of excess ( $>1$  TL)  $\text{CaF}_2$ . In a second step the succeeding  $\text{CaF}_2$  layers are grown at lower temperatures ( $300\text{--}600^\circ\text{C}$ ). The inhomogeneous morphology of the initial film allows us to study simultaneously the growth of  $\text{CaF}_2$  on the  $\text{CaF}$  interfacial layer and on  $\text{CaF}_2$  covered terraces formed during the first growth step. At low temperatures, the  $\text{CaF}_2$  growth on  $\text{CaF}_2$  tends to be layer-by-layer while the growth on the pure  $\text{CaF}$  layer is dominated by three-dimensional islands. At temperatures above  $500^\circ\text{C}$ , a transition from terrace to step nucleation is observed. These observations are explained using kinetic growth models to determine the diffusion barriers on both the  $\text{CaF}$  interfacial layer and the  $\text{CaF}_2$  islands.

### I. INTRODUCTION

Most commercial semiconductor applications are based on silicon. Although Si technology is very sophisticated, there is no insulating material which grows epitaxially on Si available for mass production. Up to now  $\text{SiO}_2$  has been used for insulating layers in most devices, but due to the amorphous structure of  $\text{SiO}_2$  it is impossible to produce multilayer heterosystems with epitaxial quality directly.  $\text{CaF}_2$  is a well suited candidate for epitaxial insulating layers on Si on account of its small lattice mismatch (0.6% at room temperature) and high band gap of 12 eV. High-quality metal-insulator heterostructures can be grown with  $\text{CaF}_2$  on Si so that nanoelectronic devices (e.g., resonant tunnelling diodes<sup>1</sup> and transistors<sup>2</sup>) can be manufactured.

In addition to technology, the system  $\text{CaF}_2/\text{Si}(111)$  also serves as a model system for the growth of ionic crystals on covalent bound semiconductors.<sup>3,4</sup> In particular the interface structure was investigated extensively with medium energy ion scattering,<sup>5</sup> x-ray standing waves,<sup>6,7</sup> x-ray photoelectron diffraction (XPD),<sup>8,9</sup> and x-ray diffraction.<sup>10–12</sup> A rough distinction may be made between two different interface structures depending on the growth temperature. At growth temperatures below  $\sim 650^\circ\text{C}$ , the first layer exhibits a bulklike stoichiometry ( $\text{CaF}_2$ -type interface). If the growth temperature is increased above  $\sim 650^\circ\text{C}$ , the  $\text{CaF}_2$  molecules are partially dissociated and the  $\text{CaF}$ -type interface is formed. The interface structure does not change sharply with the growth temperature but smoothly over a temperature range of about  $100^\circ\text{C}$ . In the case of the  $\text{CaF}_2$ -type interface, the interfacial layer consists of bulklike  $\text{CaF}_2$  adsorbed on the Si with weak Si-F bonds. The  $\text{CaF}$ -type interface consists of one  $\text{CaF}$  layer with strong Si-Ca bonds.<sup>13</sup> Low-energy electron microscopy investigations by Tromp and Reuter<sup>14</sup> showed that the  $\text{CaF}_2$ -type interface is unstable under certain growth conditions, while the  $\text{CaF}$ -type is the more stable one.

Due to the high quality of the  $\text{CaF}$ -type interface, we used a two-step growth process for the experiments presented in this report: first we grew the  $\text{CaF}$  interface layer by evapo-

rating 1.3 triple layers (TL's)  $\text{CaF}_2$  at  $T_1 = 750^\circ\text{C}$ . One TL corresponds to one molecular  $\text{CaF}_2$  layer consisting of one Ca layer embedded between two fluorine layers. Further layers were grown in a second step at the temperature  $T_2 < T_1$ . The interfacial  $\text{CaF}$  layer is closed before the subsequent  $\text{CaF}_2$  growth starts on it. This is confirmed previous by x-ray photoelectron diffraction (XPD),<sup>15</sup> and atomic force microscopy (AFM) investigations.<sup>16</sup> Excess  $\text{CaF}_2$  which is not incorporated into the interfacial  $\text{CaF}$  layer leads to the formation of  $\text{CaF}_2$  islands confined to substrate terraces. Thus the surface exhibits two different terrace types after the first growth step: (i) terraces covered by one  $\text{CaF}$ -layer only, and (ii) terraces where the interfacial  $\text{CaF}$ -layer is covered additionally by the excess  $\text{CaF}_2$  (see Fig. 1). The formation of this morphology is described in more detail in Ref. 16.

In order to predict the growth mode for a certain set of growth parameters (growth temperature, deposition rate, and substrate morphology) using kinetic growth models, one has to know the diffusion barrier heights for the diffusion of the ad molecules on the substrate. In our case we have to distinguish between two different diffusion barriers for the growth during the second growth step. First, the  $\text{CaF}$  interfacial layer forms an effective substrate with the diffusion constant  $D_{\text{CaF}}$

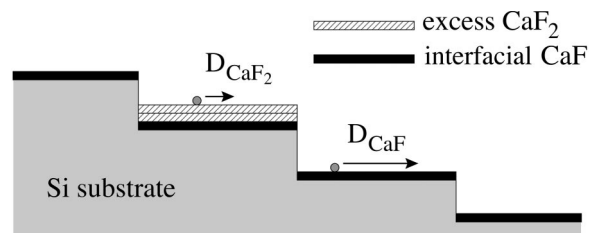


FIG. 1. Schematic drawing of the 1.3 TL thick  $\text{CaF}_2$  film morphology after the first growth step at  $T_1 = 750^\circ\text{C}$ . Due to the high deposition temperature the Si substrate is covered entirely by the interfacial  $\text{CaF}$  layer (black). Excess  $\text{CaF}_2$  (hatched) forms 2 TL thick islands on 20% of the terraces of the  $\text{CaF}$  wetting layer. This template structure forms the effective substrate for the second growth step. The arrows indicate the two different diffusion constants  $D_{\text{CaF}_2}$  and  $D_{\text{CaF}}$  on the different materials.

for the subsequent growth of bulklike  $\text{CaF}_2$ . Second, diffusion of the ad molecules deposited on the  $\text{CaF}_2$  islands is governed by the diffusion constant  $D_{\text{CaF}_2}$ . It is obvious that the two diffusion constants should be different due to the chemical differences between the bulklike  $\text{CaF}_2$  islands with pure ionic bonds and the interfacial  $\text{CaF}$  layer with mixed ionic and covalent bonds. For instance, in contrast to the interfacial  $\text{CaF}$  layer a  $\text{CaF}_2(111)$  layer has no dipole moment.

Most of the previous studies concerning the growth kinetics of  $\text{CaF}_2$  on  $\text{Si}(111)$  were carried out at high temperatures where the  $\text{CaF}$ -type interface is formed during the early stages of adlayer growth. Using the two-step growth process it is possible to study the growth of  $\text{CaF}_2$  on the interfacial  $\text{CaF}$ - $\text{Si}$  layer at various temperatures without altering the structure of the interfacial layer even below the formation temperature for the reacted  $\text{CaF}$ -layer. Further, the coexistence between  $\text{CaF}$ - and  $\text{CaF}_2$ -terminated areas due to the excess  $\text{CaF}_2$  before the second growth step enables us to investigate simultaneously the  $\text{CaF}_2$  growth on the interfacial  $\text{CaF}$  layer and the bulklike  $\text{CaF}_2$  islands at low temperatures ( $T < 650^\circ\text{C}$ ).

## II. EXPERIMENTAL SETUP

The  $\text{CaF}_2$  films were grown in a ultrahigh vacuum (UHV) system equipped with a  $\text{CaF}_2$  evaporator, a mass spectrometer for residual gas analysis, and a spot-profile analysis low-energy electron diffraction (SPA-LEED) instrument. LEED was used only to check the preparation of the  $\text{Si}(111)-7 \times 7$  before the  $\text{CaF}_2$  deposition in order to avoid electron-beam-induced damage in the  $\text{CaF}_2$  films.<sup>7,17,18</sup> The  $\text{CaF}_2$  is evaporated with a homemade e-beam evaporator using a tantalum crucible. The deposition rate is controlled with a quartz microbalance. After the growth process the samples were transferred *in situ* into a second UHV chamber equipped with an atomic force microscope (AFM).<sup>19</sup> The homemade AFM is based on the laser deflection scheme<sup>20</sup> and operated in the contact mode. The noise level of the AFM in the vertical direction is about 0.05 nm and the lateral resolution is limited by the tip radius ( $\sim 10$  nm).

The samples were cut from a  $\text{Si}(111)$  wafer with a misorientation angle of  $0.6^\circ$ . They were heated by direct electrical current flowing in the  $[1\bar{1}0]$  direction (parallel to the steps). Due to the direction of the heating current parallel to the steps we observed step bunches after removal of the native oxide by flash annealing the sample up to  $1250^\circ\text{C}$  for  $\sim 10$  s. The step bunches have an average height of 2 nm and they are separated by  $\sim 200$  nm wide terraces. Temperatures above  $700^\circ\text{C}$  were measured using an optical pyrometer calibrated at the  $\text{Si}(111)-7 \times 7$  to  $1 \times 1$  phase-transition temperature observed by LEED at  $830^\circ\text{C}$ . Lower temperatures than  $700^\circ\text{C}$  were determined using an infrared pyrometer. The estimated temperature measurement error of  $\pm 10^\circ\text{C}$  for temperatures above  $700^\circ\text{C}$  increases for lower temperatures (e.g.,  $\pm 50^\circ\text{C}$  at  $300^\circ\text{C}$ ).

## III. EXPERIMENTAL RESULTS

The  $\text{CaF}_2$  films were prepared in two growth steps. First, we deposited 1.3 TL  $\text{CaF}_2$  at  $T_1 = 750^\circ\text{C}$  with a deposition

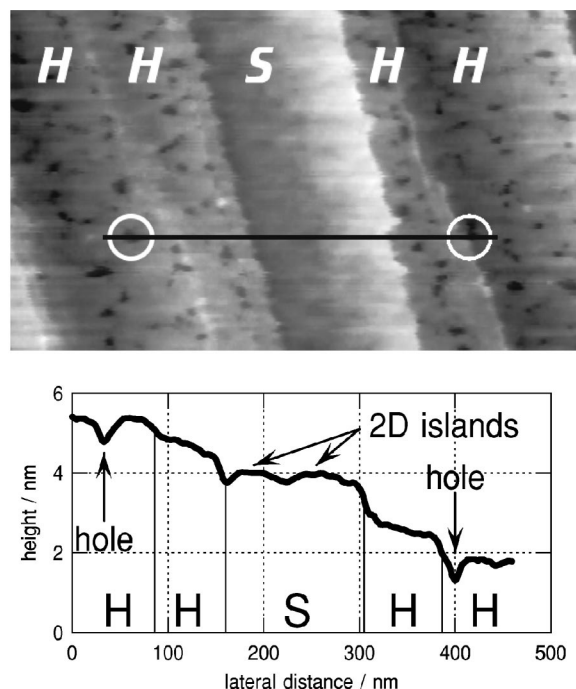


FIG. 2. 4.9 TL  $\text{CaF}_2$  grown on  $\text{Si}(111)$  at  $T_2 = 300^\circ\text{C}$  with the two-step growth process. Two types of terraces can be distinguished in the upper image: *type-H* with holes and *type-S* without holes. The scan size is  $690 \times 405$  nm<sup>2</sup>. The image was obtained under ambient conditions. The bottom image shows the height profile of the black line in the top image. The two holes ( $\sim 0.6$  nm deep) in the height profile are marked with white circles in the micrograph. The height profile of the *type-S* terrace shows two 2D islands with 0.3 nm height.

rate  $R_1$  of 0.1 TL/min. Further  $\text{CaF}_2$  was deposited in a second growth step at  $T_2 < T_1$  and a deposition rate of  $R_2 = 0.3 \dots 0.4$  TL/min immediately (1 ... 2 min) after the first step. Throughout this report the  $\text{CaF}_2$  film thickness denotes the entire film thickness deposited in *both* growth steps. The high-temperature  $T_1$  and the low deposition rate  $R_1$  in the first step were chosen to ensure that the whole  $\text{Si}$  surface is covered with  $\text{CaF}$ .

An AFM micrograph of a 4.9 TL's  $\text{CaF}_2$  film grown at  $T_2 = 300^\circ\text{C}$  with the two-step process is shown in Fig. 2. Although the whole  $\text{Si}$  surface is covered with  $\text{CaF}_2$  the step bunches of the substrate are still clearly visible. Two types of terraces can be distinguished in the image: terraces with many small holes (*type-H*) and terraces without holes (*type-S*). About 80% of the terraces are covered with these holes. The hole density on the *type-H* terraces is  $(450 \pm 40) \mu\text{m}^{-2}$  and they are on average 0.6 nm (2 TL) deep. The measurement of the hole depth is restricted due to their small diameter, which is in the same order of magnitude as the AFM tip diameter. Thus the holes could even be deeper than the measured 0.6 nm. The hole depth shows that the growth mode on the *type-H* terraces is multilayer and the holes are caused by coalesced three-dimensional islands. The *type-S* terraces are smooth apart from two-dimensional (2D) islands (cf. height profile in Fig. 2) indicating that the growth mode is layer-by-layer on the *type-S* terraces.

The average distance between the *type-S* terraces is  $\sim 1 \mu\text{m}$ . This distance corresponds to the distance between

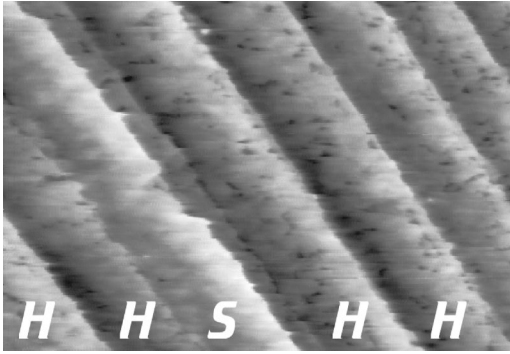


FIG. 3. 5.3 TL  $\text{CaF}_2$  grown on Si at  $T_2=400^\circ\text{C}$  with the two-step growth process. As in Fig. 2 the *type-H* and *type-S* terraces can be distinguished. The scan size is  $1300\times 900\text{ nm}^2$ . The image was obtained under ambient conditions.

the  $\text{CaF}_2$  covered terraces formed by the excess  $\text{CaF}_2$  during the first growth step (see above). It is well known that  $\text{CaF}_2$  islands growing at high temperatures on the interfacial  $\text{CaF}$  layer are two layers thick (compare Refs. 4,15,16). Combining this result with the *type-S* terrace coverage of 20% leads to an excess  $\text{CaF}_2$  amount of 0.4 TL which is in good agreement with the  $(1.3\pm 0.2)$  TL  $\text{CaF}_2$  deposited in the first growth step as determined by the quartz microbalance (1 TL for the interfacial layer plus 0.3 TL excess  $\text{CaF}_2$ ). Therefore, one can conclude that the two different film morphologies after the second growth step are caused by growth on two different effective substrates prepared in the first growth step. On the one hand, the  $\text{CaF}_2$  terraces with holes are grown directly on the pure  $\text{CaF}$  interfacial layer during the second growth step. On the other hand, the pinhole-free terraces are grown on terraces already overgrown by excess  $\text{CaF}_2$  during the first growth step. This coexistence between the two terrace types enables us to compare directly the morphology of  $\text{CaF}_2$  films grown on  $\text{CaF}_2$  and on the interfacial  $\text{CaF}$  layer under identical growth conditions.

Figure 3 shows an AFM micrograph of a 5.3 TL thick  $\text{CaF}_2$  film grown with the two-step growth process at  $T_2=400^\circ\text{C}$ . The main features (*type-H* and *type-S* terraces, amount of excess  $\text{CaF}_2$ , etc.) are the same as for the film grown at  $T_2=300^\circ\text{C}$  as described above. The hole density on the *type-H* terraces, however, is reduced to  $(210\pm 30)\mu\text{m}^{-2}$  while the average hole depth is the same as determined above for  $T_2=300^\circ\text{C}$ .

At  $T_2=500^\circ\text{C}$ , a substantial  $\text{CaF}_2$  amount nucleates at substrate steps forming long islands at these steps coexisting with smaller islands on the terraces. Further increasing the growth temperature  $T_2$  to  $600^\circ\text{C}$  leads to a drastic change in the film morphology (see Fig. 4). All the terraces are free of pinholes. In contrast to the micrographs shown before, the  $\text{CaF}_2$  film grown at  $600^\circ\text{C}$  decorates the substrate step bunches and forms a “staircase-like” structure with monomolecular steps. Most islands are formed in front of the Si substrate steps. This “staircase-like” structure is attributed to the 2 nm high step bunches produced during the sample preparation. At these enhanced growth temperatures it is not possible to distinguish between *type-H* and *type-S* terraces due to the absence of holes. Additionally to the dominating islands, which are nucleated at substrate steps, a few islands are nucleated on the terraces.

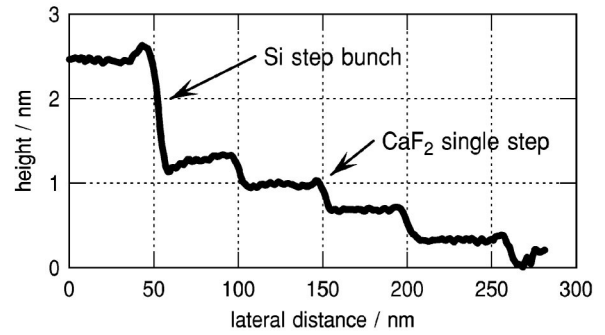
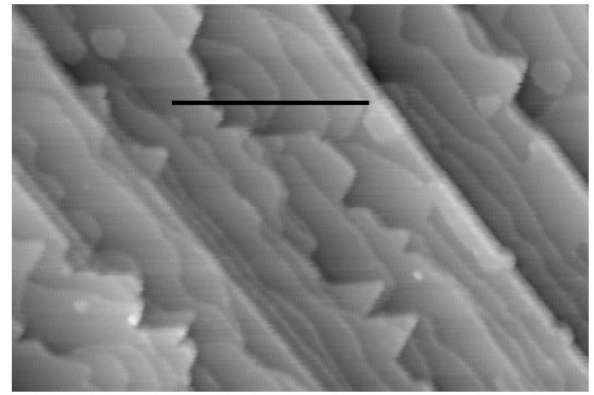


FIG. 4. 5.0 TL  $\text{CaF}_2$  grown on Si at  $T_2=600^\circ\text{C}$  with the two-step growth process. In contrast to the films grown at 300 and  $400^\circ\text{C}$  this film shows no holes. The  $\text{CaF}_2$  islands are nucleated at the substrate step bunches. The scan size of the upper image is  $800\times 550\text{ nm}^2$ . The bottom image shows a height profile of the black line in the micrograph. In the profile, one can see clearly the “staircase-like”  $\text{CaF}_2$  film with monomolecular steps nucleated at the substrates step bunch. The image was obtained *in situ*.

#### IV. GROWTH MODEL

In this section, we first introduce a growth model for the case of pure homogeneous nucleation i.e., nucleation only takes place on substrate terraces. Thereafter the influence of heterogeneous nucleation at substrate steps on the growth mode is discussed.

##### A. Homogeneous nucleation on terraces

The experimental results can be explained by the following growth model which is based on the models developed by Tersoff *et al.*<sup>21</sup> for the case of homoepitaxial growth and its extension to heteroepitaxial growth by Olmstead *et al.*<sup>4,22</sup>

The growth stage at which the second layer starts to nucleate, is crucial for the transition from three-dimensional (3D) to layer-by-layer growth. If the first layer is completed before second layer islands nucleate, the growth mode is layer-by-layer. Otherwise the nucleation of the second layer starts before the first layer islands coalesce and one obtains 3D island growth. There is a critical island radius  $R_c$  of the first layer islands where second layer islands nucleate on top of the first layer islands. The probability for second layer nucleation increases rapidly for first layer islands with a radius  $R > R_c$ . For a vanishing “Ehrlich-Schwoebel barrier” and a smallest stable island size of two molecules (corresponding to a critical nucleus size of one molecule), the critical island radius  $R_c$  is<sup>21</sup>

$$R_c = \left( \frac{192 L_n^2 a^2 D_{\text{CaF}_2}}{\pi F} \right)^{1/8}, \quad (1)$$

where  $a^2$  denotes the surface unit-cell area,  $D_{\text{CaF}_2}$  the diffusion constant of  $\text{CaF}_2$  admolecules on first layer  $\text{CaF}_2$  islands, and  $F$  the incident flux per unit cell.  $L_n$  denotes half of the distance between the first layer islands and can be expressed by<sup>23</sup>

$$L_n = \left( a^2 \frac{4D_x}{F} \right)^{1/6}, \quad (2)$$

where  $D_x$  denotes the  $\text{CaF}_2$  diffusion constant on the effective substrate after the first growth step. Since in our case the surface has two different top layers after the first growth step, one has to distinguish between the growth on *type-H* and *type-S* terraces during the second growth step. These different terrace types act as different effective substrates for the subsequent growth in the second step. For *type-H* terraces the  $\text{CaF}_2$  admolecules of the first layer diffuse on the pure interfacial  $\text{CaF}$  layer ( $D_x = D_{\text{CaF}}$ ). In the case of the *type-S* terraces, the  $\text{CaF}_2$  molecules already diffuse on excess  $\text{CaF}_2$  ( $D_x = D_{\text{CaF}_2}$ ).

If  $R_c$  exceeds  $L_n$ , one expects layer-by-layer growth, because second layer islands nucleate after the coalescence of the first layer islands. For  $R_c < L_n$  the film grows in the multilayer or 3D island growth mode, because the nucleation of second layer islands starts before the coalescence of the first layer islands.

Using Eqs. (1) and (2) one can compute the ratio  $R_c/L_n$

$$\frac{R_c}{L_n} = \left( \frac{48 D_{\text{CaF}_2}}{\pi D_x} \right)^{1/8} = \left( \frac{48}{\pi} \right)^{1/8} e^{-\Delta E/(8kT)} \quad (3)$$

assuming  $D_x = a^2 \nu \exp(-E_x/[kT])$  with hopping barrier heights  $E_x = E_{\text{CaF}_2}$  and  $E_x = E_{\text{CaF}}$  corresponding to the diffusion constants  $D_{\text{CaF}_2}$  and  $D_{\text{CaF}}$ , respectively.  $\Delta E = E_{\text{CaF}_2} - E_x$  denotes the difference between the diffusion barrier heights on the first layer islands ( $E_{\text{CaF}_2}$ ) and on the effective substrate ( $E_x$ ). It is assumed here that the hopping attempt frequency  $\nu$  is the same for diffusion on both substrates.

Taking  $R_c = L_n$  as criterion for the transition from 3D to layer-by-layer growth, one can compute the corresponding transition temperature  $T_c$

$$T_c = \frac{\Delta E}{k \ln(48/\pi)}. \quad (4)$$

The transition temperature depends only on the difference between the diffusion barriers on the substrate and the first layer islands and is independent of the deposition flux  $F$ .

The calculations for the critical island radius  $R_c$  were carried out for circular shaped islands. For the transition criterion  $R_c = L_n$  used above one expects pinholes between the circular islands. Therefore, real layer-by-layer growth where the first layer is completely closed before second layer nucleation implies that  $fR_c = L_n$ . This ‘‘shape-factor’’  $f$  depends on the actual island shape and the lateral arrangement of the islands. Since circular islands have the most compact shape, we conclude that  $f \leq 1$  for the shape factor. Further, due to fluctuations of the island separations, the transition between

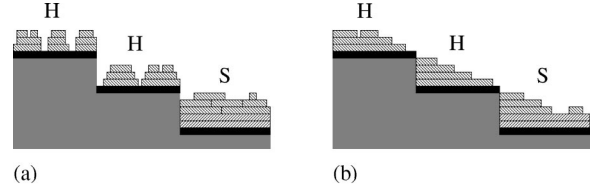


FIG. 5. Schematic drawing of the observed growth modes: (a) 3D island and layer-by-layer growth on *type-H* and *type-S* terraces, respectively, (b) growth of the ‘‘staircase-like’’ structure in the step nucleation regime.

both growth modes is not as sharp as described by this theory. Taking these limitations into account, Eq. (4) is an upper limit for the transition temperature or lower limit for the diffusion barrier difference  $\Delta E$  for a given transition temperature  $T_c$  determined by experimental observations.

## B. Heterogeneous nucleation at steps

Increasing the growth temperature  $T_2$  leads to larger diffusion lengths of the  $\text{CaF}_2$  admolecules on the effective substrate. If the diffusion length and the terrace width  $w$  have the same order of magnitude, one has to take heterogeneous nucleation at substrate steps into account. To describe the step nucleation we use a model originally developed by Myers-Beaghton and Vvedensky<sup>24</sup> which has been used before to describe the growth modes of  $\text{CaF}_2$  on vicinal  $\text{CaF-Si}(111)$  by Olmstead *et al.*<sup>4,22</sup>

Myers-Beaghton and Vvedensky introduced the dimensionless parameter  $\alpha = w^2 a^2 F / D$  to describe the influence of nucleation at steps<sup>24</sup> with average terrace width  $w$ . This parameter represents the ratio of the average time one admolecule needs to diffuse towards a step ( $w^2/D$ ) and the time to deposit one monolayer ( $1/[Fa^2]$ ). For  $\alpha > 1$  the growth is dominated by nucleation on the terraces as described above, while for  $\alpha < 1$  step nucleation starts to compete with the terrace nucleation. Thus, the transition from terrace to step nucleation occurs at  $\alpha = 1$  (compare the discussions in Refs. 22 and 24) so that we can evaluate the transition temperature  $T_s$  between the two regimes:

$$T_s = \frac{E_x}{k \ln[\nu/(w^2 F)]}. \quad (5)$$

Of course, the choice of  $\alpha = 1$  as an exact value for the transition is quite arbitrary. We introduce it here to compare the results of this study concerning the growth of  $\text{CaF}_2$  on  $\text{CaF-Si}(111)$  with previous results.<sup>22,25</sup>

## V. DISCUSSION

Both models discussed in the previous section determine critical temperatures for the transition either from layer-by-layer to 3D island growth or from terrace to step nucleation (see also Fig. 5). Both phenomena have been observed during the second growth step of  $\text{CaF}_2$  on the effective substrate prepared in the first growth step. Since the critical temperatures depend on the diffusion barriers, we will discuss and compare these diffusion barriers for the growth of  $\text{CaF}_2$  on the two different effective substrates (the  $\text{CaF}$  interfacial layer, and terraces covered with excess  $\text{CaF}_2$ ).

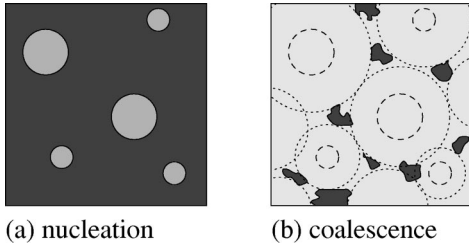


FIG. 6. Schematic drawing of the hole formation process. (a) shows the nucleation of islands (bright) on the effective substrate (dark). (b) shows the formation of the holes (dark) due to the coalescence of the growing islands. The dashed circles show the positions of the nucleated islands shown in (a). The dotted circles indicate the growth fronts of the islands.

### A. Nucleation on terraces

During the second growth step we have to distinguish between growth on two different effective substrates. First, growth on the excess  $\text{CaF}_2$  (*type-S* terraces) with  $D_x = D_{\text{CaF}_2}$ , and, second growth on the pure interfacial  $\text{CaF}$  layer (*type-H* terraces) with  $D_x = D_{\text{CaF}}$ . The first case corresponds to  $\text{CaF}_2$  homoepitaxy ( $D_x = D_{\text{CaF}_2} \Rightarrow R_c = L_n$ ) and one obtains layer-by-layer growth independent of the growth temperature  $T_2$ . The two-dimensional  $\text{CaF}_2$  islands coalesce and form a closed layer before the next layer nucleates. This process continues for the growth of higher layers so that  $\text{CaF}_2$  grows in the layer-by-layer growth mode on *type-S* terraces. Therefore, *type-S* terraces show continuous smooth films with occasional 2D islands depending on the exact coverage. In the second case ( $D_x = D_{\text{CaF}} \neq D_{\text{CaF}_2}$ ) the growth mode depends on the temperature and on the difference  $\Delta E$  between the diffusion barrier  $E_x = E_{\text{CaF}}$  on the effective substrate and  $E_{\text{CaF}_2}$  on the overgrowing  $\text{CaF}_2$  islands. According to our model we expect layer-by-layer growth for  $\Delta E \leq 0$  (corresponding to  $E_{\text{CaF}_2} \leq E_{\text{CaF}}$ ) for all growth temperatures. If  $\Delta E$  is positive the growth mode depends on the temperature. In this case we expect layer-by-layer growth for temperatures  $T_2$  above the transition temperature  $T_c$  [see Eq. (4)]. Below this temperature the growth mode switches to the growth of 3D islands.

The multilayer growth mode on *type-H* terraces leads to the formation of 3D islands. During the coalescence of these islands the observed holes are formed (cf. the model in Fig. 6). Thus the nucleation of the second  $\text{CaF}_2$  layer starts on top of first layer islands before the first layer islands coalesce for  $T_2 < T_c$ . Increasing the growth temperature also increases the spacing  $L_n$  between the islands nucleating on the  $\text{CaF}$  layer, leading to the growth of larger islands and thus to a reduction of the island and hole density as observed.

The observation of the 3D island growth mode on the *type-H* terraces can be explained by our growth model only if  $\Delta E > 0$ . Otherwise we should observe layer-by-layer growth without any formation of holes on *type-H* and *type-S* terraces. Therefore, we can conclude immediately that  $E_{\text{CaF}} < E_{\text{CaF}_2}$ .

Denlinger *et al.* calculated the hopping barriers of  $\text{CaF}_2$  admolecules on the interfacial layer.<sup>15</sup> The calculated surface corrugation potential depends on the effective charge of the Ca atoms in the interfacial layer. According to their calcula-

tions the diffusion barrier  $E_{\text{CaF}_2}$  of  $\text{CaF}_2$  admolecules on bulk  $\text{CaF}_2$  of about 1.6 eV is reduced to about  $E_{\text{CaF}} = 1.4$  eV on the  $\text{CaF}$  interfacial layer where the charge of the Ca atoms is lower than in bulk  $\text{CaF}_2$ .

From our observations we deduce that the transition temperature  $T_c$  for the transition from 3D island to layer-by-layer growth is above 400 °C. We were not able to determine the upper limit for  $T_c$  exactly, because at temperatures above 500 °C a substantial amount of  $\text{CaF}_2$  nucleated at the substrate steps. Taking the discussion of Eq. (4) into account as well, we conclude that the diffusion barrier difference  $\Delta E$  must be at least 0.16 eV using  $T_c = 400$  °C and a maximum value  $f = 1$  for the shape factor. A smaller shape factor would lead to a larger diffusion barrier difference  $\Delta E$ . This result is consistent with the value of 0.2 eV for  $\Delta E$  calculated by Denlinger *et al.*<sup>15</sup> and the range of 0.1–0.7 eV reported by Olmstead in Ref. 4.

### B. Transition to step nucleation

Up to this point in the discussion we have neglected the existence of substrate steps. To explain the drastic changes in the film morphology observed for temperatures above  $\sim 500$  °C we have to take into consideration the fact that a substantial amount of the  $\text{CaF}_2$  admolecules nucleates at substrate steps. Again, we have to consider the different diffusion barriers for the growth on the *type-H* and *type-S* terraces. The AFM micrographs show that the transition between terrace and step nucleation occurs between 500 °C and 600 °C on *type-H* terraces with 200 nm width. Using  $T_s^H = (550 \pm 50)$  °C as the transition temperature Eq. (5) results in a diffusion barrier height of  $E_{\text{CaF}} = (1.5 \pm 0.1)$  eV for the  $\text{CaF}_2$  diffusion on the  $\text{CaF}$  interfacial layer (assuming  $10^{13}$  Hz for the attempt frequency  $\nu$ ).<sup>22</sup> This result is in good agreement with the value of 1.4 eV observed by Hessinger *et al.*<sup>22</sup> using the same criterion ( $\alpha = 1$ ) to compute the diffusion barrier of  $\text{CaF}_2$  on the  $\text{CaF}$  interfacial layer from transmission electron microscopy experiments.

In the previous section we calculated a lower limit of 0.16 eV for the diffusion barrier difference  $\Delta E$  between the barriers  $E_{\text{CaF}}$  and  $E_{\text{CaF}_2}$  on the interfacial  $\text{CaF}$  layer and the  $\text{CaF}_2$  islands, respectively. This leads to a barrier height  $E_{\text{CaF}_2} \geq (1.66 \pm 0.1)$  eV for the diffusion of the  $\text{CaF}_2$  admolecules on  $\text{CaF}_2$  islands.

The diffusion barrier  $E_{\text{CaF}_2}$  can be cross checked calculating the temperature  $T_s^S$  for the transition from terrace to step nucleation on *type-S* terraces. From Eq. (5) we obtain  $T_s^B \geq (650 \pm 50)$  °C. This transition temperature is consistent with the experimental observation that the  $\text{CaF}_2$  film grows almost perfectly in the step-flow mode at  $T_2 = 600$  °C since only very few free standing islands are observed on the terraces (compare Fig. 4). Therefore, we conclude that  $E_{\text{CaF}_2} = (1.7 \pm 0.1)$  eV.

## VI. CONCLUSIONS

Summarizing, we investigated the morphology of ultrathin  $\text{CaF}_2$  films grown on vicinal  $\text{Si}(111)$  substrates using a two-step growth process. The different temperatures for the second growth step enable us to study the growth kinetics of

CaF<sub>2</sub> on the interfacial CaF layer formed at high temperatures over a wide temperature range. At lower temperatures the growth on the pure interfacial CaF layer is dominated by the coalescence of three-dimensional islands while the growth mode on CaF<sub>2</sub> precovered terraces is layer-by-layer. Increasing the growth temperature of the second growth step results in a drastically changed film morphology which is attributed to the transition from terrace to step nucleation. The islands consisting of excess CaF<sub>2</sub> deposited in the first growth step were used to compare the growth on the free CaF interfacial layer to the growth on these CaF<sub>2</sub> islands under identical growth conditions. The growth mode on the excess CaF<sub>2</sub> double layers in the second growth step is layer-by-layer even for the lowest temperatures used here. This behavior is consistently explained by kinetic growth models. The differences between the CaF<sub>2</sub> growth modes on the interfacial CaF and on the bulklike CaF<sub>2</sub> are caused by the different diffusion constants of the admolecules on these dissimilar materials.

The results concerning the growth kinetics of CaF<sub>2</sub>/Si(111) presented here are consistent with most of the studies previously reported by other authors for one-step growth procedures<sup>4,15,25</sup> but there are quantitative differences concerning the diffusion constants. In contrast to previous investigations, the use of AFM enabled us to observe *directly* the morphology of the ultrathin CaF<sub>2</sub> films with high lateral resolution. For the transition temperature of the transition

from layer-by-layer to 3D island growth on the substrate terraces and the transition from step to terrace nucleation observed here we were able to determine the diffusion barriers. The diffusion barrier for CaF<sub>2</sub> molecules on the CaF interfacial layer is estimated as  $E_{CaF} = (1.5 \pm 0.1)$  eV, while the barrier for the diffusion on the CaF<sub>2</sub> islands is higher [ $E_{CaF_2} = (1.7 \pm 0.1)$  eV]. Using these values for the diffusion barriers and the growth models presented here leads to a consistent explanation of our observations and also of experimental results presented previously by other groups<sup>4</sup> and calculations by Denlinger *et al.*<sup>15</sup> These calculations led to  $E_{CaF_2} = 1.6$  eV and  $E_{CaF} = 1.4$  eV as upper limits of the diffusion barriers. The lower diffusion barrier on the CaF is caused by the different charge distribution in the interfacial layer compared to the bulk CaF<sub>2</sub>.

For the future we plan investigations of the CaF<sub>2</sub> growth on well-oriented Si(111) substrates. Larger terrace widths  $w$  lead to higher transition temperatures  $T_s$  between terrace and step nucleation. If the transition temperature  $T_s$  for terrace-step nucleation exceeds the transition temperature  $T_c$  for 3D/layer-by-layer growth one should be able to observe the predicted transition between 3D island and layer-by-layer growth using substrates with lower miscut angles. Further, we intend to carry out Monte Carlo simulations to investigate the role of the diffusion barrier difference  $\Delta E$  in heteroepitaxy.

\*Corresponding author. Fax: +49 511 762 4877. Electronic address: klust@fkp.uni-hannover.de

<sup>1</sup>T. Suemasu, M. Watanabe, J. Suzuki, Y. Kohno, M. Asada, and N. Suzuki, *Jpn. J. Appl. Phys., Part 1* **33**, 57 (1994).

<sup>2</sup>K. Mori, W. Saitoh, T. Suemasu, Y. Kohno, M. Watanabe, and M. Asada, *Physica B* **227**, 213 (1996).

<sup>3</sup>L.J. Schowalter, R.W. Fathauer, R.P. Goehner, R.W. DeBlois, S. Hashimoto, J.-L. Peng, W.M. Gibson, and J.P. Krusius, *J. Appl. Phys.* **58**, 302 (1985).

<sup>4</sup>M. A. Olmstead, in *Thin Films: Heteroepitaxial Systems*, edited by A. W. K. Liu and M. Santos (World Scientific, Singapore, in press).

<sup>5</sup>R.M. Tromp and M.C. Reuter, *Phys. Rev. Lett.* **61**, 1756 (1988).

<sup>6</sup>J. Zegenhagen and J.R. Patel, *Phys. Rev. B* **41**, 5315 (1990).

<sup>7</sup>J. Wollschläger, T. Hildebrandt, R. Kayser, J. Viernow, A. Klust, J. Bätjer, A. Hille, T. Schmidt, and J. Falta, *Appl. Surf. Sci.* (to be published).

<sup>8</sup>J.D. Denlinger, E. Rotenberg, U. Hessinger, M. Leskovar, and M.A. Olmstead, *Appl. Phys. Lett.* **62**, 2057 (1993).

<sup>9</sup>E. Rotenberg, J.D. Denlinger, M. Leskovar, U. Hessinger, and M.A. Olmstead, *Phys. Rev. B* **50**, 11 052 (1994).

<sup>10</sup>C.A. Lucas and D. Loretto, *Appl. Phys. Lett.* **60**, 2071 (1992).

<sup>11</sup>C.A. Lucas, G.C.L. Wong, and D. Loretto, *Phys. Rev. Lett.* **70**, 1826 (1993).

<sup>12</sup>K.G. Huang, J. Zegenhagen, J.M. Phillips, and J.R. Patel, *Phys. Rev. Lett.* **72**, 2430 (1994).

<sup>13</sup>M.A. Olmstead, R.I.G. Uhrberg, R.D. Bringans, and R.Z. Bachrach, *Phys. Rev. B* **35**, 7526 (1987).

<sup>14</sup>R.M. Tromp and M.C. Reuter, *Phys. Rev. Lett.* **73**, 110 (1994).

<sup>15</sup>J. Denlinger and E. Rotenberg, *Phys. Rev. B* **51**, 5352 (1995).

<sup>16</sup>A. Klust, H. Pietsch, and J. Wollschläger, *Appl. Phys. Lett.* **73**, 1967 (1998).

<sup>17</sup>K. Miura, K. Sugiura, and H. Sugiura, *Surf. Sci. Lett.* **253**, L407 (1991).

<sup>18</sup>R. Bennowitz, D. Smith, and M. Reichling, *Phys. Rev. B* **59**, 8237 (1999).

<sup>19</sup>G. Binnig and C.F. Quate, *Phys. Rev. Lett.* **56**, 930 (1986).

<sup>20</sup>G. Meyer and N.M. Amer, *Appl. Phys. Lett.* **53**, 1045 (1988).

<sup>21</sup>J. Tersoff, A.W.D. van der Gon, and R.M. Tromp, *Phys. Rev. Lett.* **72**, 266 (1994).

<sup>22</sup>U. Hessinger, M. Leskovar, and M.A. Olmstead, *Phys. Rev. Lett.* **75**, 2380 (1995).

<sup>23</sup>L.-H. Tang, *J. Phys. I* **3**, 935 (1993).

<sup>24</sup>A.K. Myers-Beaghton and D.D. Vvedensky, *Phys. Rev. B* **42**, 5544 (1990).

<sup>25</sup>J. Wollschläger, H. Pietsch, and A. Klust, *Appl. Surf. Sci.* **130-132**, 29 (1998).